

NEW DESIGN AND COMPARATIVE STUDY VIA TWO TECHNIQUES FOR WIND ENERGY CONVERSION SYSTEM

Introduction. With the advancements in the variable speed direct drive design and control of wind energy systems, the efficiency and energy capture of these systems is also increasing. As such, numerous linear controllers have also been developed, in literature, for MPPT which use the linear characteristics of the wind turbine system. The major limitation in all of those linear controllers is that they use the linearized model and they cannot deal with the nonlinear dynamics of a system. However, real systems exhibit nonlinear dynamics and a nonlinear controller is required to handle such nonlinearities in real-world systems. **The novelty** of the proposed work consists in the development of a robust nonlinear controller to ensure maximum power point tracking by handling nonlinearities of a system and making it robust against changing environmental conditions. **Purpose.** In the beginning, sliding mode control has been considered as one of the most powerful control techniques, this is due to the simplicity of its implementation and robustness compared to uncertainties of the system and external disturbances. Unfortunately, this type of controller suffers from a major disadvantage, that is, the phenomenon of chattering. **Methods.** So in this paper and in order to eliminate this phenomenon, a novel non-linear control algorithm based on a synergetic controller is proposed. The objective of this control is to maximize the power extraction of a variable speed wind energy conversion system compared to sliding mode control by eliminating the phenomenon of chattering and have a good power quality by fixing the power coefficient at its maximum value and the Tip Speed Ratio maintained at its optimum value. **Results.** The performance of the proposed nonlinear controllers has been validated in MATLAB/Simulink environment. The simulation results show the effectiveness of the proposed scheme, suppression of the chattering phenomenon and robustness of the proposed controller compared to the sliding mode control law. References 33, table 1, figures 17. **Key words:** synergetic controller, sliding mode controller, maximum power point tracking, macro-variable, wind energy conversion system.

Вступ. З досягненнями у проектуванні та керуванні вітряними енергосистемами з регульованою швидкістю, зростають також ефективність та захоплення енергії цих систем. Так, в літературі також розроблено численні лінійні контролери для відстеження точки максимальної потужності, які використовують лінійні характеристики системи з вітряними турбінами. Основним обмеженням у всіх цих лінійних контролерах є те, що вони використовують лінеаризовану модель і не можуть мати справу з нелінійною динамікою системи. Однак реальні системи демонструють нелінійну динаміку, і для обробки таких нелінійностей у реальних системах необхідний нелінійний контролер. **Новизна** запропонованої роботи полягає у розробці надійного нелінійного контролера для забезпечення відстеження точки максимальної потужності шляхом обробки нелінійності системи та забезпечення її стійкості до змін умов навколишнього середовища. **Мета.** Спочатку управління ковзним режимом вважалось одним з найпотужніших методів управління, що пов'язано з простотою його реалізації та надійністю порівняно з невизначеністю системи та зовнішніми збуреннями. На жаль, цей тип контролера страждає від головного недоліку, а саме явища вібрування. **Методи.** Тому у цій роботі з метою усунення цього явища пропонується новий нелінійний алгоритм управління, заснований на синергетичному контролері. Завдання цього контролю – максимізувати відбір потужності системи перетворення енергії вітру зі змінною швидкістю порівняно із регулюванням ковзного режиму, усуваючи явище вібрування, і мати хорошу якість енергії, фіксуючи коефіцієнт потужності на його максимальному значенні та підтримуючи кінцевий коефіцієнт швидкості на його оптимальному значенні. **Результати.** Ефективність запропонованих нелінійних контролерів перевірена в середовищі MATLAB/Simulink. Результати моделювання показують ефективність запропонованої схеми, придушення явища вібрування та стійкість запропонованого контролера порівняно із законом управління ковзного режиму. Бібл. 33, табл. 1, рис. 17.

Ключові слова: синергетичний контролер, контролер ковзного режиму, відстеження точки максимальної потужності, макрозмінна, система перетворення енергії вітру.

1. Introduction. Nowadays, most countries of the world are facing difficulties in using conventional sources for power generation due to exhaustion of fossil fuels and environmental issues like air pollution and greenhouse gases. For these reasons, energy producers are heading to the use of renewable energy sources (sun, wind, biomass, etc) to produce electricity. These new energies appear today as a solution to energy production problems in the world [1, 2]. As a renewable energy source, wind energy is one of the most promising renewable energy resources for generating electricity due to its cost competitiveness compared to other conventional types of energy resources.

A wind energy conversion system (WECS) can be separated into three main conversion stages, including the transformation from the wind kinetic energy to the rotational mechanical energy in the wind turbine, the transformation from the turbine mechanical energy to the electrical energy by an electrical generator, and the connection between the electrical generator and the power grid by an electronic

power converter [3]. The generated energy can be used either for standalone loads or fed into the power grid through an appropriate power electronic interface [4].

In WECS, several types of electric generators are used such as squired-cage induction generator, doubly fed induction generator [5]. Lately, with the advances of power electronic technology, permanent magnet synchronous generator based variable speed WECS are becoming more popular over other types of generators which are used in wind energy systems because of advantages such as its simple structure, ability of operation at low velocities, self-excitation capability leading to high power factor and high efficiency operation [6], moreover permanent magnet synchronous motor can be connected directly to the turbine without system of gearbox [7]. According to Betz's law, only 59.3 % of total available wind energy can be converted into mechanical energy considering no mechanical losses in the system [8]

and in most cases about 20-60 % of the Betz's limit can be obtained from wind turbines [9].

However, the conventional way to get the maximum power from wind is based on the optimum mathematical relationship. The turbine output power is a function of rotor speed if the wind speed is assumed to be constant. Thus controlling the rotor speed allows control over power production from the generator [10]. There are several other mathematical relationships suitable for maximum power tracking. In many cases electromagnetic torque vs. power relation is used to obtain the maximum power [11].

Basically, the studied maximum power point tracking (MPPT) methods for WECSs include three strategies:

1. Relying on wind speed measurement used by tip speed ratio (TSR) method;
2. Relying on wind turbine power curve used by power signal feedback and optimal torque control methods;
3. Relying on hill climb search of wind turbine power curve without any knowledge about this curve used by perturb and observe method [12].

Control design, in WECS is becoming a challenging task due to the nonlinear dynamics and uncertainties present in these systems [13]. The requirements of the control system include tracking a speed reference, generated by MPPT, by controlling the rotational speed in a variable speed wind turbine system [14, 15], while the most important part of the control design for nonlinear dynamical systems is to guarantee the stability.

Conventional control methods are based on proportional-integral (PI) regulators, which were initially developed for linear systems, and their design is limited by the parameters tuning, which is delicate and requires adjustment in a changing environment due to random variations of the power source [16]. Different model based control systems, such as sliding mode, known for its simplicity, speed and robustness was widely adopted and has shown its effectiveness in many applications.

Unfortunately, this type of controller suffers from a major disadvantage, that is, the phenomenon of chattering. The chattering phenomenon occurs due to implementation issues of the sliding mode control signal in digital devices operating with a finite sampling frequency, where the switching frequency of the control signal cannot be fully implemented [17].

In order to eliminate this phenomenon, a more recent technique (synergistic approach) is proposed in [18], the synergetic control method presents a suitable option to control nonlinear uncertain systems operating in disturbed environments. That's why several studies have been conducted in this field.

In this study, we adopted the tip speed ratio control strategy with a non-linear control algorithm based on a sliding mode theory and synergetic controller in order to maximize the power extraction of a variable speed of WECS. The main aspect of control design is definition of a macro-variable for synergetic control and sliding surface for sliding mode control.

In [19, 20] synergetic control is proposed as a nonlinear control technique to track photovoltaic systems and it is shown using simulation that synergetic control eliminates chattering effect compared to sliding mode

control. The synergetic controller which has received much attention for photovoltaic systems can also be designed for WECS.

In our paper, the motivation is to use a nonlinear synergetic control of the wind speed turbine in order to operate at maximum power extraction. This new approach does not require the linearization of the model and explicitly uses a nonlinear model to design the control law.

The aim of paper is to optimize the power produced by a wind energy system under varying conditions based on two maximum power point tracking techniques.

The rest of the paper is organized as follows. The modeling of all parts of the wind speed turbine and problem formulation for MPPT to extract the maximum power are presented in Section 2. The synergetic and sliding mode control theory is summarized in Section 3, followed by the design of the synergetic controller and sliding mode. Simulation results and comparison with two well known controllers, sliding mode controller and synergetic controller, are presented in Section 4. Conclusion is given in Section 5.

2. Wind turbine modeling. WECS includes various multidisciplinary subsystems which can be classified as aerodynamic, structural and electrical. The aerodynamic subsystem represents the aerodynamic model of the wind turbine. The structural subsystems include blades, tower and drive train models. The electrical subsystems include the generator, the back-to-back converter and the system control models.

Model of wind turbine. The wind speed can be modelled as a deterministic sum of harmonics with frequency in range of 0.1–10 Hz as follows [21]:

$$V(t) = V_0 \left(1 + \sum_{n=1}^i A_n \sin \omega_n t \right), \quad (1)$$

where V_0 is the average wind speed; A_n is the magnitude of n^{th} kind of eigenswing, ω_n is the eigenfrequency of n^{th} kind of eigenswing excited in the turbine rotating.

The aerodynamic (mechanical) power developed by a wind turbine is given by the following expression [22, 23]:

$$P_{aer} = \frac{1}{2} \cdot C_p(\lambda, \beta) \cdot \rho \cdot \pi \cdot R^2 \cdot V^3, \quad (2)$$

where ρ is the air density, kg/m^3 ; R is the radius of the turbine blade, m; V is the wind speed, m/s; $C_p(\lambda, \beta)$ is the power coefficient which is a function of both a factor λ known as the tip speed ratio (TSR) and blade pitch angle β (deg).

TSR is defined as the ratio of the turbine's blade-tip speed to the wind velocity, and can be expressed as:

$$\lambda = \frac{R \cdot \Omega_t}{V}, \quad (3)$$

where Ω_t is the rotor speed of a wind turbine, rad/s.

Several numerical expressions exist for $C_p(\lambda, \beta)$. Here the used relation is given by [24]:

$$C_p(\lambda, \beta) = (0.5 - 0.0167(\beta - 2)) \cdot \sin\left(\frac{\pi(\lambda + 0.1)}{18 - 0.3(\beta - 2)}\right) - 0.00184(\lambda - 3)(\beta - 2), \quad (4)$$

The C_p curve is shown in Fig. 1, from which there is an optimum λ at which the power coefficient C_p is maximal.

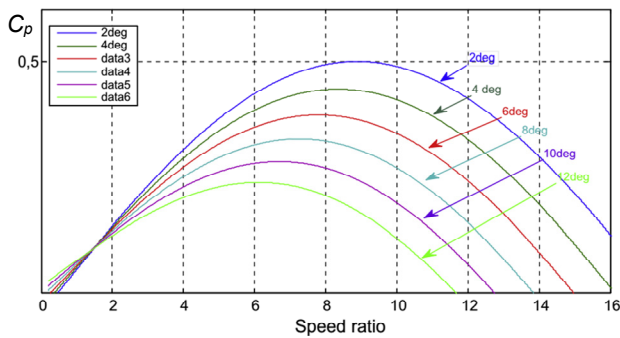


Fig. 1. Power coefficient $C_p(\lambda, \beta)$ versus tip-speed ratio for various values of β

The value of the power coefficient C_p is a function of λ and β , it reaches the maximum at the particular λ named λ_{opt} . Hence, to maximize the extracted energy of wind turbine λ should be maintained at λ_{opt} with the optimal rotor speed of the turbine which is determined from (3) and given as

$$\Omega_{ref} = \frac{\lambda_{opt} \cdot V}{R}, \quad (5)$$

where Ω_{ref} is the rotor speed reference, rad/s.

For a constant β Fig. 2 illustrates that there is only one fixed value of TSR ($\lambda_{opt} = 9.14$) for which C_p is maximum ($C_{pmax} = 0.5$). This special value λ_{opt} is known as the optimal peak speed ratio, it can be expressed by:

$$\lambda_{opt} = \frac{\Omega_{ref} \cdot R}{V}. \quad (6)$$

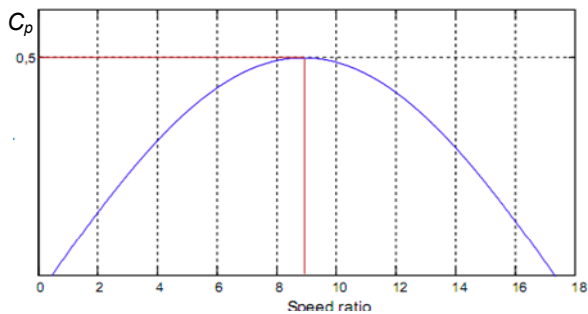


Fig. 2. Power coefficient C_p versus λ at fixed β

Gear box model. The role of gear box is to transform the mechanical speed of the turbine to the generating speed, and the aerodynamic torque to the gear box torque according to the following mathematical formulas [25]:

$$\begin{cases} T_g = T_{aer} / G; \\ \Omega_{tur} = \Omega / G; \\ T_{aer} = P_{aer} / \Omega_{tur}, \end{cases} \quad (7)$$

and the mechanical equation of the shaft, including both the turbine and the generator masses, is given by [24]:

$$J \frac{d\Omega}{dt} = T_g - T_{em} - f \cdot \Omega, \quad (8)$$

where Ω is the mechanical generator speed; Ω_{tur} is the speed of the turbine; T_g is the torque applied on the shaft of turbine; T_{aer} is the aerodynamic torque; P_{aer} is the aerodynamic power; T_{em} is the electromagnetic torque; J is the total moment of inertia; f is the viscous friction coefficient; G is the gear box ratio.

The system of equations (1)-(8) permit to us to construct the block diagram of the wind turbine as shown on Fig. 3 [32, 33].

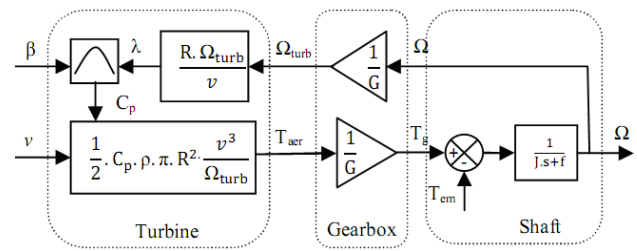


Fig. 3. Wind turbine block diagram.

3. MPPT control strategies. According to Fig. 1, for a particular value of tip speed ratio λ_{opt} , C_p has a unique maximum value at which maximum power is captured from wind by the wind turbine. As a result, to achieve power efficiency maximization, the turbine tip speed ratio must be sustained at its optimum value in spite of wind variations. Also, for a given wind velocity, there is an optimal value for rotor velocity which maximizes the power supplied by the wind. That is equally saying, the turbine system realizes the MPPT function [26]. Consequently, the system can operate at the peak of the $P(\Omega)$ curve, and the maximum power is extracted continuously from the wind. That is illustrated in Fig. 4.

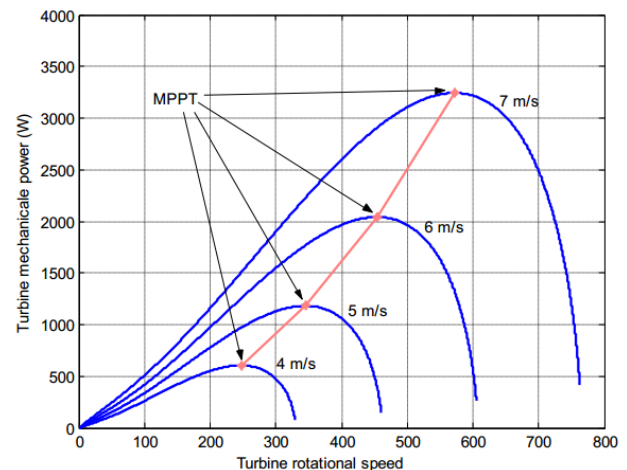


Fig. 4. Turbine powers various speed characteristics for different wind speeds with indication of the MPPT curve

So the MPPT technique consists of varying turbine speed constantly according to wind speed variations, so that the tip speed ratio is maintained in its optimum value, thus the power generation is optimum. In order to extract the maximum power from the wind, we adopted the speed turbine control strategy. It permits to carry the speed of the wind turbine into the desired value which corresponds to the maximum power point. The wind turbine speed control scheme is represented in Fig. 5, where C_Ω is the speed controller.

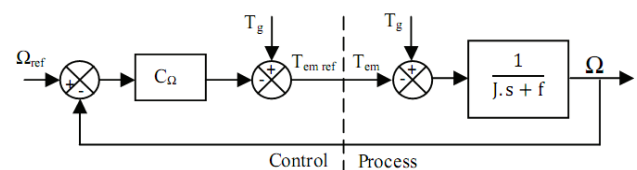


Fig. 5. Speed generator feedback control

This control structure consists to adjust the torque appearing on the turbine shaft in order to fix the turbine speed at a reference that permits to track of the maximum wind power. In this study, we assume that the electromagnetic torque equals to its reference all the time [24].

$$T_{em} = T_{em-ref} . \quad (9)$$

Controller design based to sliding mode. Sliding mode control is one of the non-linear techniques. It is a particular operation mode of variable structure control systems. Its concept consists of moving the state trajectory of the system to a predetermined surface called sliding surface and maintaining it around this latter with an appropriate logic commutation [27]. The design of sliding mode controller is done in three steps [29, 30]:

1. Selection of the sliding surface;
2. Establishing the conditions of existence and convergence;
3. Determination of the control law.

The sliding surface is given by [31]:

$$S(x) = \left(\frac{d}{dt} + \lambda_{sm} \right)^{r-1} \cdot e(x), \quad (10)$$

where λ_{sm} is the positive constant indicating the desired control bandwidth; r is the relative degree, equal to the number of times to derive the output to appear the command; $e(x)$ is the error between the variable and its reference.

For $n = 1$ the error as being the sliding surface:

$$e(\Omega) = \Omega_{ref} - \Omega , \quad (11)$$

where Ω_{ref} is the desired speed.

This surface derivative is:

$$\dot{e}(\Omega) = \dot{\Omega}_{ref} - \dot{\Omega} . \quad (12)$$

Combining the previous equation with equation (8), we obtain:

$$\dot{e}(\Omega) = \dot{\Omega}_{ref} + \frac{1}{J} (-T_g + T_{em} + f \cdot \Omega), \quad (13)$$

The controller structure includes two parts, one part on the exact linearization and another said stabilizing [26-28], so:

$$T_{em} = T_{em}^{eq} + T_{em}^n . \quad (14)$$

Substituting the expression of the control speed by their expressions given in (13), the equations below are defined as follow:

$$\dot{e}(\Omega) = \dot{\Omega}_{ref} + \frac{1}{J} (-T_g + (T_{em}^{eq} + T_{em}^n) + f \cdot \Omega). \quad (15)$$

During the sliding mode and in permanent regime, we have:

$$e(\Omega) = 0; \quad \dot{e}(\Omega) = 0; \quad T_{em}^n = 0 .$$

Where the equivalent control is:

$$T_{em}^{eq} = -J \cdot \dot{\Omega}_{ref} - f \cdot \Omega + T_g . \quad (16)$$

Therefore, the correction factor is given by:

$$T_{em}^n = -k \cdot \text{sgn} e(\Omega), \quad (17)$$

where k is a positive constant.

The control expression:

$$T_{em} = -J \cdot \dot{\Omega}_{ref} - f \cdot \Omega + T_g - k \cdot \text{sgn} e(\Omega). \quad (18)$$

Controller design based to synergetic control.

Synergetic control is a state space approach for the design of control for complex highly connected nonlinear systems [20]. It forces the system state variables to evolve on a designer chosen invariant manifold enabling for desired performance to be achieved despite uncertainties and disturbances without damaging chattering inherent to the sliding mode technique [20]. Synergetic synthesis begins with the definition of the macro-variable based on the equations of the state space. For the macro-variable, it can be expressed as follows:

$$\psi = \psi(x, t). \quad (19)$$

The objective of the synergetic controller is to operate the controlled system on the manifold for which the macro-variable is null $\psi = 0$.

The expected dynamic evolution of the macro-variable is given as a function of:

$$T \dot{\psi} + \psi = 0, \quad T > 0 . \quad (20)$$

where the derivative of the total macro-variable is noted by $\dot{\psi}$, and T is a parameter design which designates the convergence rate from the closed loop system to the manifold that is to be specified by $\psi = 0$.

Finally, the control law (evolution in time of the control output) is synthesized according to equation (14) and the dynamic model of the system.

According to synergetic controller, we will select the first set of macro-variables as equation (20):

$$\psi = \Omega_{ref} - \Omega . \quad (21)$$

This derivative is:

$$\dot{\psi} = \dot{\Omega}_{ref} - \dot{\Omega} . \quad (22)$$

Combining equations (8), (20), and (21), we get the electromagnetic torque as the following control law:

$$T_{em-ref} = T_{em} = \frac{J}{T} \left[\frac{T \cdot f}{J} \Omega - \frac{T \cdot T_g}{J} + (\Omega_{ref} - \Omega) \right]. \quad (23)$$

4. Simulation results. In this section we evaluate the performances and effectiveness of the control strategies by simulating the wind turbine under the turbulent wind speed profile of Fig. 6.

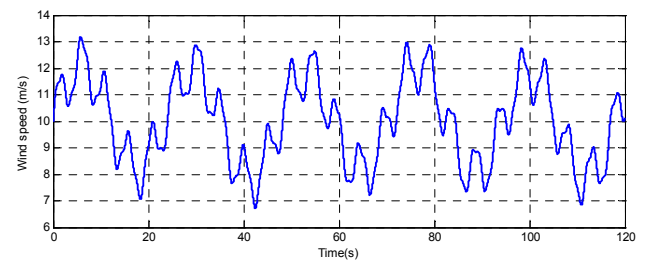


Fig. 6. Wind speed profile

The system parameters that have been chosen for the wind turbine are given in the Table 1.

Table 1

Wind turbine parameters

Parameters	Values
Density of air, kg/m ³	1.22
Radius of rotor, m	3
Gear box ratio	1
Turbine total inertia, kg·m ²	16
Total viscous friction coefficient, N·m/s	0.06

The sliding surface and power coefficient are shown in Fig. 7-9 respectively. For sliding mode controller, good tracking capability was observed but it is perturbed by the high-frequency oscillations (the chattering) which can cause instability and damage to the system and there are no oscillations around the C_{pmax} for synergetic controller.

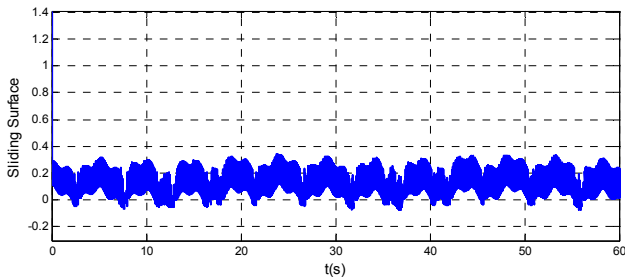


Fig. 7. Sliding surface

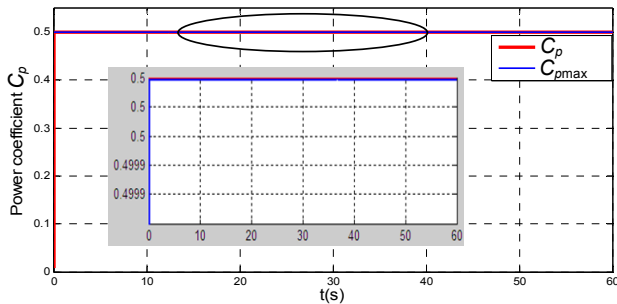


Fig. 8. Power coefficient using synergetic control

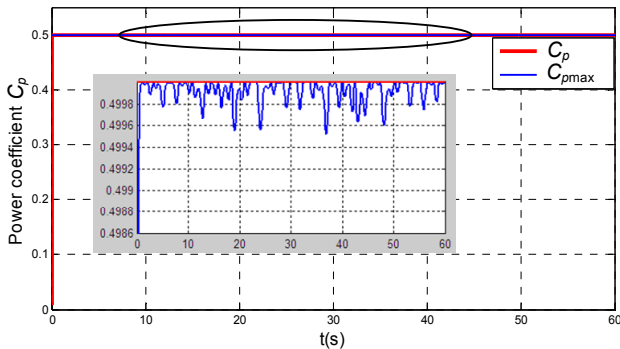


Fig. 9. Power coefficient using sliding mode

Figures 10, 11 show that the TSR follows its reference very well corresponding to the maximum and optimal value TSR $\lambda_{opt} = 9.14$ for both controllers, but with sliding mode controller the appearance of high chattering effect is always present.

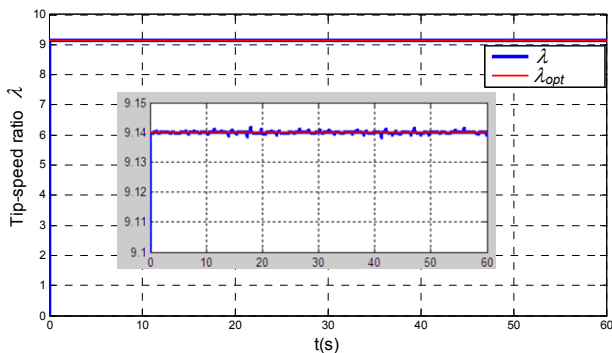


Fig. 10. Tip-speed ratio using synergetic control

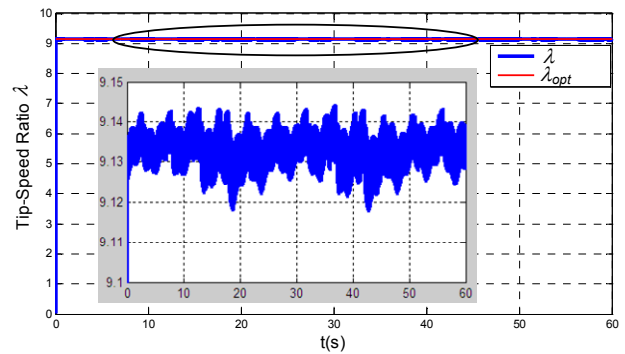


Fig. 11. Tip-speed ratio using sliding mode

According to Fig. 12, 13 the variation of the mechanical speed is adapted to the variation of the wind, which shows the direct influence of the wind on the speed of rotation of the shaft, we also note that the mechanical speed perfectly follows its reference value for the two controllers. But a zoom on these graphs shows that there is an error between the speed of rotation and its reference with the sliding mode controller. This confirms the effectiveness and good performance of the synergetic controller.

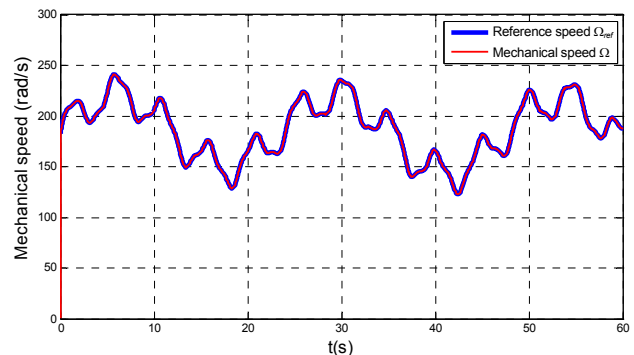


Fig. 12. Mechanical speed using synergetic control

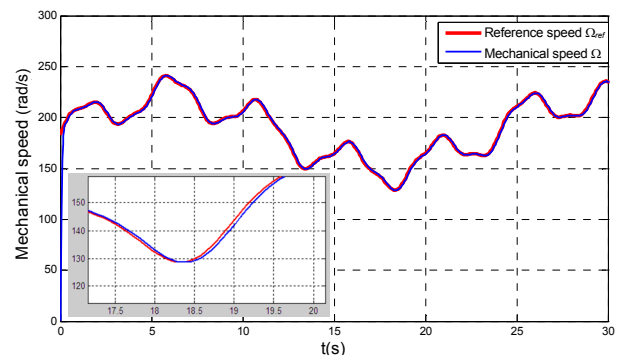


Fig. 13. Mechanical speed using sliding mode

Figures 14, 15 show the response of aerodynamic power. It is clear that the produced power follows well its optimal reference with good dynamics and track perfectly the reference for the two controllers, which means that the maximum power point can be achieved despite fast-varying wind velocity.

We can clearly see that in Fig. 16, 17 the macro-variable function and sliding mode surface equals zero, which shows that the controller parameters are properly chosen. But as we can see, Fig 16 the high chattering effect on the sliding surface.

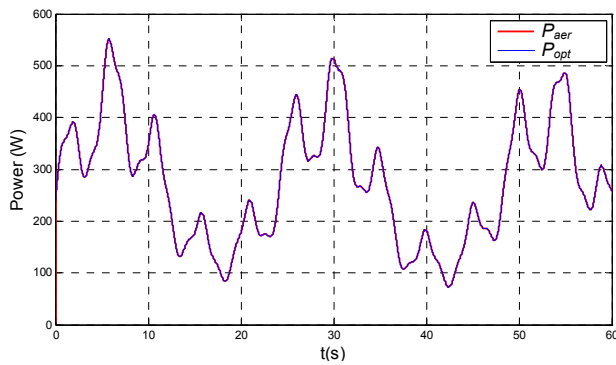


Fig. 14. Aerodynamic power using synergetic control

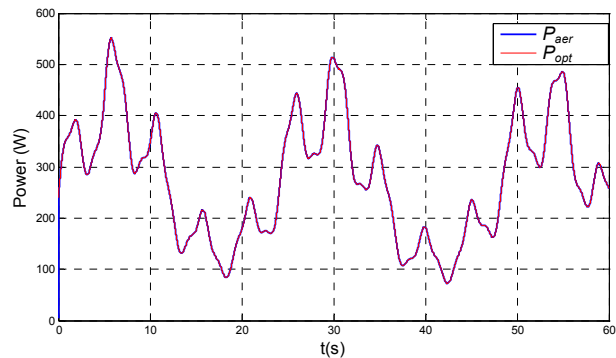


Fig. 15. Aerodynamic power using sliding mode

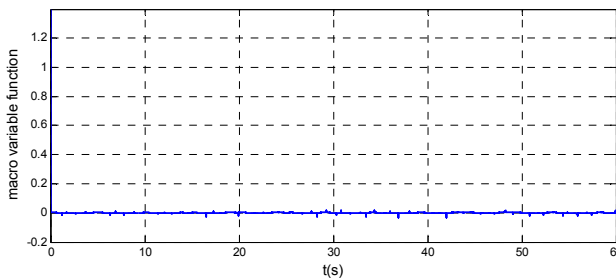


Fig. 16. Macro-variable function

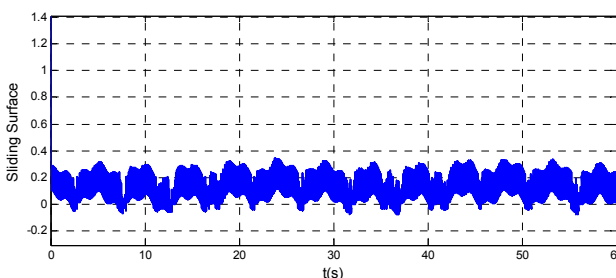


Fig. 17. Sliding surface function

From these results, we noticed that the MPPT controller based on synergetic is the most efficient technique compared to the sliding mode controller. It achieves maximum power with more stability, precision and better response time, with more trajectory tracking. However, the sliding mode method requires slow response time, with more oscillations and a chattering effect. For that, it can be stated that the synergetic control is a robust and efficient approach; it has better performance and a good dynamic response under variable wind speed conditions.

5. Conclusions.

In this paper, two maximum power point tracking strategies techniques are developed and compared to

optimize the power produced by a wind energy system under varying conditions. According to the performance analysis of each method, it can be concluded that the maximum power point tracking controller based on synergetic control allows determining and tracking the maximum power point with more efficiency, fast response and high reliability compared to other controllers based on sliding mode. The main advantage of the synergetic controller, compared to the sliding mode, is the good reference tracking, the suppression of the chattering phenomenon and the reduction of the overshoot. The effectiveness and the robustness to external disturbances, noise and uncertainty parameters are shown in the simulation results.

Conflict of interest. The authors declare no conflict of interest.

REFERENCES

- Jeong H., Lee K., Choi S., W. Choi. Performance improvement of LCL-filter-based grid-connected inverters using PQR power transformation. *IEEE Transactions on Power Electronics*, 2010, vol. 25, no. 5, pp. 1320-1330. doi: <https://doi.org/10.1109/tpe.2009.2037225>.
- Lee J.-S., Jeong H.-G., Lee K.-B. Active damping for wind power systems with LCL filters using a DFT. *Journal of Power Electronics*, 2012, vol. 12, no. 2, pp. 326-332. doi: <https://doi.org/10.6113/jpe.2012.12.2.326>.
- Bounar N., Labdai S., Boulkroune A., Farza M., M'Saad M. Adaptive fuzzy control scheme for variable-speed wind turbines based on a doubly-fed induction generator. *Iranian Journal of Science and Technology, Transactions of Electrical Engineering*, 2020, vol. 44, no. 2, pp. 629-641. doi: <https://doi.org/10.1007/s40998-019-00276-6>.
- Agarwal V., Aggarwal R.K., Patidar P., Patki C. A novel scheme for rapid tracking of maximum power point in wind energy generation systems. *IEEE Transactions on Energy Conversion*, 2010, vol. 25, no. 1, pp. 228-236. doi: <https://doi.org/10.1109/tec.2009.2032613>.
- Rolan A., Luna A., Vazquez G., Aguilar D., Azevedo G. Modeling of a variable speed wind turbine with a permanent magnet synchronous generator. *2009 IEEE International Symposium on Industrial Electronics*, 2009, pp. 734-739. doi: <https://doi.org/10.1109/isie.2009.5218120>.
- Chan T., Lai L.L. Permanent-magnet machines for distributed power generation: a review. *2007 IEEE Power Engineering Society General Meeting*, 2007, pp. 1-6. doi: <https://doi.org/10.1109/PES.2007.385575>.
- Jlassi I., Estima J.O., Khojet El Khil S., Mrabet Bellaaj N., Marques Cardoso A.J. Multiple open-circuit faults diagnosis in back-to-back converters of PMSG drives for wind turbine systems. *IEEE Transactions on Power Electronics*, 2015, vol. 30, no. 5, pp. 2689-2702. doi: <https://doi.org/10.1109/TPEL.2014.2342506>.
- Bouderbala M., Bossoufi B., Lagrioui A., Taoussi M., Aroussi H.A., Ihedrane Y. Direct and indirect vector control of a doubly fed induction generator based in a wind energy conversion system. *International Journal of Electrical and Computer Engineering*, 2019, vol. 9, no. 3, pp. 1531-1540. doi: <https://doi.org/10.11591/ijece.v9i3.pp1531-1540>.
- He Q., Zhang F., Liu D., Gao C., Shi S., Xi P. Analysis on the development status and problems of China's offshore wind power. *2018 2nd IEEE Conference on Energy Internet and Energy System Integration (EI2)*, 2018, pp. 1-4. doi: <https://doi.org/10.1109/EI2.2018.8582177>.
- Worke M.Y., Abido M.A. Maximum Power Control of DFIG Based Grid Connected Wind Turbine Generator System. *Renewable Energy and Power Quality Journal*, 2018, vol. 1, pp. 444-449. doi: <https://doi.org/10.24084/repqj16.344>.
- Boukhezzer B., Lupu L., Siguerdidjane H., Hand M. Multivariable control strategy for variable speed, variable pitch

- wind turbines. *Renewable Energy*, 2007, vol. 32, no. 8, pp. 1273-1287. doi: <https://doi.org/10.1016/j.renene.2006.06.010>.
12. Wang Q., Chang L. An intelligent maximum power extraction algorithm for inverter-based variable speed wind turbine systems. *IEEE Transactions on Power Electronics*, 2004, vol. 19, no. 5, pp. 1242-1249. doi: <https://doi.org/10.1109/TPEL.2004.833459>.
13. Toulabi M., Bahrami S., Ranjbar A.M. An Input-to-State Stability Approach to Inertial Frequency Response Analysis of Doubly-Fed Induction Generator-Based Wind Turbines. *IEEE Transactions on Energy Conversion*, 2017, vol. 32, no. 4, pp. 1418-1431. doi: <https://doi.org/10.1109/TEC.2017.2696510>.
14. Kumar D., Chatterjee K. A review of conventional and advanced MPPT algorithms for wind energy systems. *Renewable and Sustainable Energy Reviews*, 2016, vol. 55, pp. 957-970. doi: <https://doi.org/10.1016/j.rser.2015.11.013>.
15. Lee S.-W., Chun K.-H. Adaptive Sliding Mode Control for PMSG Wind Turbine Systems. *Energies*, 2019, vol. 12, no. 4, p. 595. doi: <https://doi.org/10.3390/en12040595>.
16. Li S., Haskew T.A., Xu L. Conventional and novel control designs for direct driven PMSG wind turbines. *Electric Power Systems Research*, 2010, vol. 80, no. 3, pp. 328-338. doi: <https://doi.org/10.1016/j.epsr.2009.09.016>.
17. Pratap B., Singh N., Kumar V. Robust Control of Variable Speed Wind Turbine Using Quasi-Sliding Mode Approach. *Procedia Computer Science*, 2018, vol. 125, pp. 398-404. doi: <https://doi.org/10.1016/j.procs.2017.12.052>.
18. Kolesnikov A., Veselov G., Kolesnikov A. *Modern applied control theory: synergetic approach in control theory*. Moscow-Taganrog, TRTU Publ., 2000.
19. Attoui H., Khader F., Melhaoui M., Kassmi K., Essounboul N. Development and experimentation of a new MPPT synergetic control for photovoltaic systems. *Journal of Optoelectronics and Advanced Materials*, 2016, vol. 18, no. 1-2, pp. 165-173. Available at: <https://joam.inoe.ro/articles/development-and-experimentation-of-a-new-mppt-synergetic-control-for-photovoltaic-systems/> (accessed 21 May 2020).
20. Akoro E., Tevi G.J., Faye M.E., Doumbia M.L., Maiga A.S. Artificial Neural Network Photovoltaic Generator Maximum Power Point Tracking Method using Synergetic Control Algorithm. *International Journal on Emerging Technologies*, 2020, vol. 11, no. 2, pp. 590-594. Available at: <https://www.researchtrend.net/ijet/pdf/Artificial%20Neural%20Network%20Photovoltaic%20Generator%20Maximum%20Power%20Point%20Tracking%20Method%20using%20Synergetic%20Control%20Algorithm%20Edjadessamam%20AKORO%201893n7.pdf> (accessed 21 May 2020).
21. Ounnas D., Ramdani M., Chenikher S., Bouktir T. Optimal Reference Model Based Fuzzy Tracking Control for Wind Energy Conversion System. *International Journal of Renewable Energy Research*, 2016, vol. 6, no. 3, pp. 1129-1136. Available at: <https://www.ijrer.org/ijrer/index.php/ijrer/article/view/4258/pdf> (accessed 21 May 2020).
22. Aissou R., Rekioua T., Rekioua D., Tounzi A. Nonlinear predictive control of a permanent magnet synchronous generator used in wind energy. *Journal of Electrical Engineering*, 2014, vol. 14, no. 4, pp. 331-336. Available at: <http://jee.ro/articles/WN1397935592W5352cde8e8fe5.pdf> (accessed 21 May 2020).
23. Daghigh A., Javadi H., Torkaman H. Considering wind speed characteristics in the design of a coreless AFPM synchronous generator. *International Journal of Renewable Energy Research*, 2016, vol. 6, no. 1, pp. 263-270. Available at: <https://www.ijrer.org/ijrer/index.php/ijrer/article/view/3135/pdf> (accessed 21 May 2020).
24. Watson S., Moro A., Reis V., Baniotopoulos C., Barth S., Bartoli G., Bauer F., Boelman E., Bosse D., Cherubini A., Croce A., Fagiano L., Fontana M., Gambier A., Gkoumas K., Golightly C., Latour M.I., Jamieson P., Kaldellis J., Macdonald A., Murphy J., Muskulus M., Petrini F., Pigolotti L., Rasmussen F., Schild P., Schmehl R., Stavridou N., Tande J., Taylor N., Telsnig T., Wiser R. Future emerging technologies in the wind power sector: A European perspective. *Renewable and Sustainable Energy Reviews*, 2019, vol. 113, art. no. 109270. doi: <https://doi.org/10.1016/j.rser.2019.109270>.
25. Messaoud M., Abdessamed R. Modeling and optimization of wind turbine driving permanent magnet synchronous generator. *Jordan Journal of Mechanical and Industrial Engineering*, 2011, vol. 5, no. 6. Available at: <http://jjmie.hu.edu.jo/files/v5n6/JJMIE%20-77-10.pdf> (accessed 21 May 2020).
26. Errami Y., Ouassaid M., Maaroufi M. A performance comparison of a nonlinear and a linear control for grid connected PMSG wind energy conversion system. *International Journal of Electrical Power & Energy Systems*, 2015, vol. 68, pp. 180-194. doi: <https://doi.org/10.1016/j.ijepes.2014.12.027>.
27. Bennassar A., Banerjee S., Jamma M., Essalmi A., Akherraz M. Real time high performance of sliding mode controlled induction motor drives. *Procedia Computer Science*, 2018, vol. 132, pp. 971-982. doi: <https://doi.org/10.1016/j.procs.2018.05.113>.
28. Evangelista C., Valenciaga F., Puleston P. Active and reactive power control for wind turbine based on a MIMO 2-sliding mode algorithm with variable gains. *IEEE Transactions on Energy Conversion*, 2013, vol. 28, no. 3, pp. 682-689. doi: <https://doi.org/10.1109/TEC.2013.2272244>.
29. Krim Y., Abbes D., Krim S., Faouzi Mimouni M. Power management and second-order sliding mode control for standalone hybrid wind energy with battery energy storage system. *Proceedings of the Institution of Mechanical Engineers, Part I: Journal of Systems and Control Engineering*, 2018, vol. 232, no. 10, pp. 1389-1411. doi: <https://doi.org/10.1177/0959651818784320>.
30. Meng Z., Shao W., Tang J., Zhou H. Sliding-mode control based on index control law for MPPT in photovoltaic systems. *CES Transactions on Electrical Machines and Systems*, 2018, vol. 2, no. 3, pp. 303-311. doi: <https://doi.org/10.30941/CESTEMS.2018.00038>.
31. Chavira F., Ortega-Cisneros S., Rivera J. A novel sliding mode control scheme for a PMSG-based variable speed wind energy conversion system. *Energies*, 2017, vol. 10, no. 10, art. no. 1476. doi: <https://doi.org/10.3390/en10101476>.
32. Levron Y., Shmilovitz D. Maximum power point tracking employing sliding mode control. *IEEE Transactions on Circuits and Systems I: Regular Papers*, 2013, vol. 60, no. 3, pp. 724-732. doi: <https://doi.org/10.1109/TCSI.2012.2215760>.
33. Rajendran S., Jena D. Backstepping sliding mode control for variable speed wind turbine. *2014 Annual IEEE India Conference (INDICON)*, 2014, pp. 1-6. doi: <https://doi.org/10.1109/INDICON.2014.7030634>.

Received 14.04.2021

Accepted 24.05.2021

Published 25.06.2021

Mohamed Seddik Mahgoun¹, PhD Student of Electrical Engineering,

Abd Essalam Badoud¹, Associate Professor,

¹ Automatic Laboratory of Setif,

Electrical Engineering Department,

University Ferhat Abbas Setif 1,

Setif, Algeria.

e-mail: mahgounm@yahoo.fr,

badoudabde@univ-setif.dz (Corresponding author)